

Angular scattering of low-energy electrons by atomic and molecular oxygen, argon, and helium

R. C. Dehmel,* M. A. Fineman,[†] and D. R. Miller

Department of Applied Mechanics and Engineering Sciences, University of California, San Diego, La Jolla, California 92093

(Received 28 July 1975)

The differential cross sections for electrons scattered by He, O, Ar, and O₂ at 15 eV and by O and O₂ at 5 eV have been determined using a modulated crossed-beam technique. The results for He, Ar and O₂ agree well with previously published experimental and theoretical values. Measurements on O₂ extend to larger back-scattered angles than previously reported. Results for O are compared with the theoretical calculations of Thomas and Nesbet. Reasonable agreement with theory is obtained at 5 eV, and while the calculations only extend to 11.0 eV, the trend in shape appears correct at 15 eV. A small-angle dip in the cross section is observed which is not predicted by the theory.

I. INTRODUCTION

Recently we reported measurements¹ on the ratio of forward scattering to backscattering of electrons in the energy range 3–20 eV by atomic and molecular oxygen using the modulated crossed-beam technique. It was found that atomic oxygen has a strong forward scattering at the lower energies. Subsequently, Thomas and Nesbet² carried out a matrix variational calculation for electron scattering by atomic oxygen and presented integral and differential cross sections for elastic and inelastic scattering for energies of 0.14–11.0 eV. They then calculated the ratio of forward scattering to backscattering by integrating the elastic differential cross-section curves; their results are in agreement with our experiment.

Experimental measurements of the angular distribution of low-energy electrons scattered from atomic oxygen are very difficult because of the poor intensities of atomic oxygen in beam sources currently available, and because these sources always contain significant amounts of the parent molecular oxygen. However, the availability of new theoretical calculations for electron-oxygen collisions and the current interest in upper atmospheric phenomena involving these collisions seemed to warrant the attempt to make such low-energy angular measurements.

In this paper we report measurements of differential-scattering cross sections (elastic + inelastic) for electrons incident on He, O, Ar, and O₂. The data are presented as absolute differential cross sections after normalizing to available total cross sections. The work was done using the modulated crossed-beam technique at electron energies of 5 eV with O and O₂ and 15 eV with He, Ar, O, and O₂. As far as we know,³ these are the first experimental differential-scattering cross sections reported for atomic oxygen, as well as being the

first angular distributions of electrons scattering from a gas, other than H, which requires dissociation of a parent molecule to produce the atomic species. In the sections below, we will discuss the experimental apparatus and procedures, the method of data reduction, and a comparison with other published data.⁴

II. EXPERIMENTAL

A modulated crossed-beam apparatus (see Figs. 1 and 2) was used. It consists of a free-jet molecular-beam source, a monoenergetic electron-beam source, a rotatable scattered-electron detector, a primary electron-beam collector, and a quadrupole mass spectrometer for analysis of the molecular beam. The apparatus was housed in a large stainless-steel two-chamber vacuum tank whose background pressures during a run were $\sim 5 \times 10^{-5}$ torr in the source chamber and $\sim 2 \times 10^{-7}$ torr in the experimental chamber.

A. Molecular-beam source and detector

Atomic oxygen was formed by dissociation of O₂ at 15 torr in a microwave discharge, with a subsequent free-jet expansion⁵ through a 0.022-cm orifice. We had replaced the rf discharge source used in our previous work¹ by the microwave (2450-MHz) discharge source.⁶ This new source was more stable and reproducible, had less reflected power, and was easier to ignite than the rf discharge source. In addition, higher dissociation percentages (up to $\sim 50\%$) were obtainable, and fewer charged species were detectable in the main beam. Under normal operating conditions, the number of charged particles from the discharge detected by the channeltron multiplier was negligible (< 0.02 electrons/sec). The beam flux density was $\sim 10^{16}$ – 10^{17} particles/cm² sec⁻¹. At the high densities in the nozzle expansion most excited

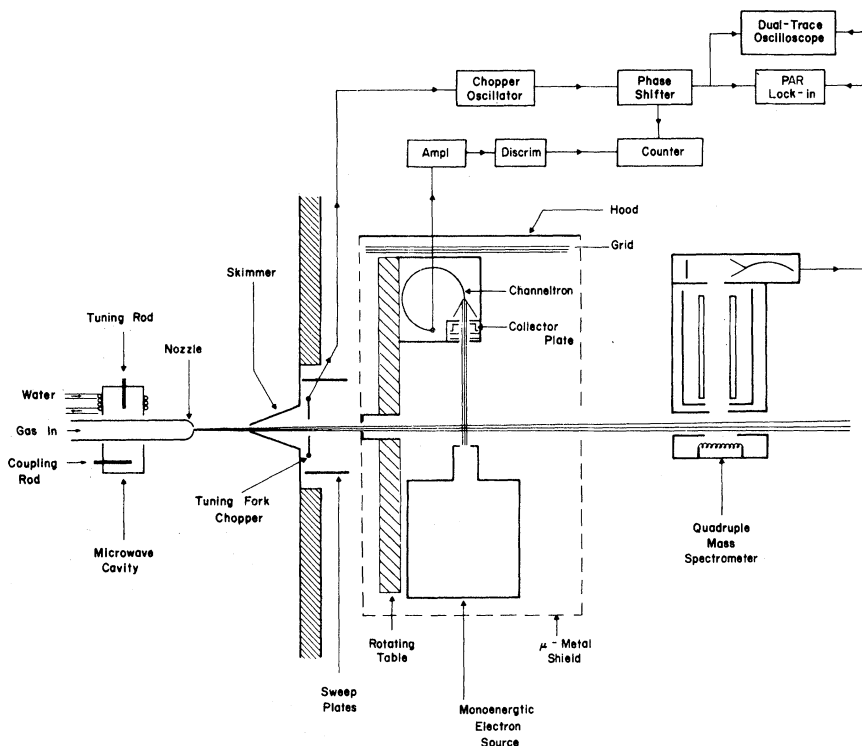


FIG. 1. Diagram of the experimental arrangement used to measure angular scattering of electrons by He, O, Ar, and O₂.

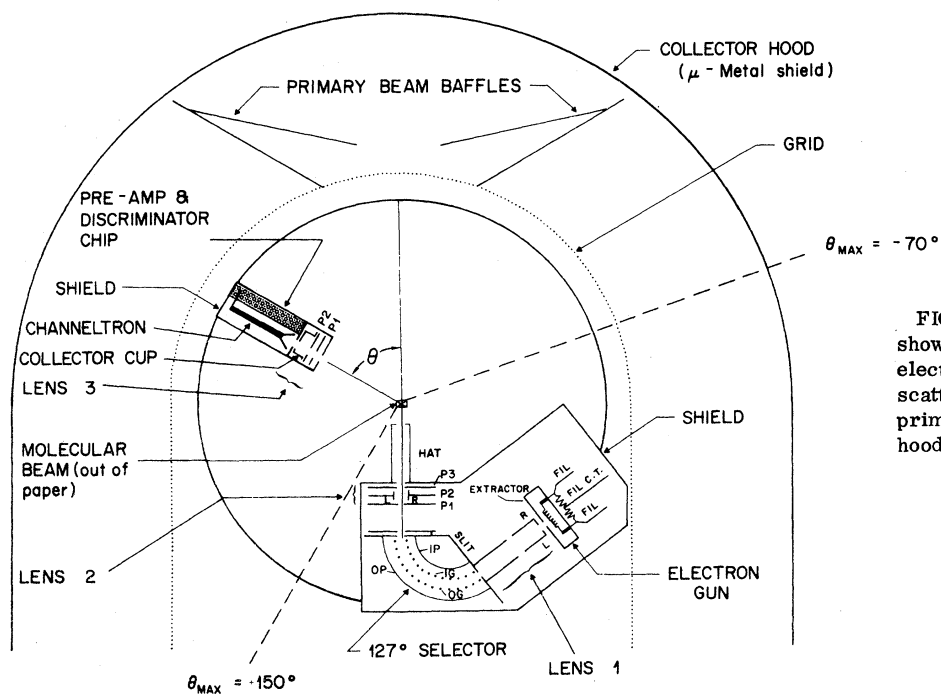


FIG. 2. Schematic diagram showing the 127° electrostatic electron energy selector, scattering electron detector, primary electron collector hood, and the collision region.

species are deexcited by collisions, and we expect that most of the excited $O(^1D)$ and $O_2(^1\Delta_g)$ would be collisionally deexcited so that the beam would be mostly ground state $O(^3P)$ and $O_2(^3\Sigma_g^-)$.⁷ At lower pressures, 0.5 torr, in flowing discharges, Falick *et al.*⁸ have measured excited-species concentrations as high as 10%. For He, Ar, and O_2 , the apparatus was run without the discharge as a simple free-jet source with typical source pressures between 15–25 torr.

The molecular beam was defined by a conical skimmer (orifice diameter = 0.53 cm) and chopped at 500 Hz by a Bulova tuning fork chopper (Fig. 1). A pair of plates (± 90 V), mounted above and below the chopper, was used to sweep out charged particles from the beam. A mask, placed at the entrance of the electron-scattering region, produced a rectangular molecular beam (0.380 cm wide by 0.318 cm high) at the interaction region with the electron beam. The molecular beam was analyzed downstream by a quadrupole mass spectrometer.

B. Monoenergetic electron beam source and collector

The electron-scattering apparatus was the same as that used by McGowan *et al.*^{9,10} but modified for the present experiment (Fig. 2). The changes made in the 127° cylindrical electrostatic energy selector were (i) the use of a spiral-wound 8-mil diam thoriated-iridium filament; (ii) the addition of an exit "hat"; and (iii) the encasement of the entire electron source in a metal shield box to prevent stray electrons from reaching the detector. All metal parts in the scattering apparatus were gold-blackened to reduce electron reflection. The scattering region was held at ground potential. The energy width of the electron beam was measured at the collector to be 120 mV using the retarding-potential technique. This figure is supported by the more extensive measurements made by McGowan *et al.*⁹ Due to contact potentials, we estimate that the energy of the primary beam is uncertain by ± 0.5 eV. The entire scattering apparatus was enclosed in a μ -metal shield which reduced the residual magnetic field inside the apparatus to less than 0.05 G.

Initially, the primary beam was collected by a Faraday cup, but it was found that large numbers of electrons remained uncollected allowing some to be detected by the channeltron multiplier and contributing to the background current and its associated noise. The cup was eliminated entirely and the wall of the μ -metal shield was insulated and then positively biased to collect the primary beam. A grounded tungsten grid was placed 10 cm in front of this "hood" to prevent field penetration

and secondary electrons from entering the scattering region.

C. Scattered-electron detector

The scattered-electron detector consisted of a lens which focused the electrons into a Bendix channeltron electron multiplier followed by an amplifier-discriminator circuit. The detector was mounted 6.4 cm from the scattering volume, subtended a solid angle of 8×10^{-4} sr with respect to the interaction zone, and could be rotated from $+152^\circ$ to -70° with respect to the primary beam (see Fig. 2). The output pulses from the discriminator were converted by a level-shifter emitter-follower circuit to negative pulses acceptable by an SSR-1110 digital synchronous computer. The dead time of the detector was 3.3 μ sec.

The SSR-1110 counter is a dual-channel device which was synchronized to the beam modulation. One channel (B) displayed the background counts with molecular beam off, chopper closed, and the other (A) the background plus scattered electron counts with the molecular beam on, chopper open. The scattered electron signal (A-B), called "D" below, is also displayed.

Rotation of the detector table was manually controlled and the angular settings were determined visually. Angles were reproducible to $\pm \frac{1}{8}^\circ$. The angles measured spanned from -70° to $+150^\circ$. Data were taken at 10° increments for Ar and He and 15° for O and O_2 . In order to increase the S/N ratios, long counting times were used; for example, the time at each angle for a "single-pass" run for Ar was 15 min and $\frac{1}{2}$ h for O and O_2 . Ion gauges and the mass-spectrometer ionizer were turned off during the electron-scattering measurements.

For O and O_2 , "multipass" runs (sweeping forward and backward through the angles a number of times) were made until signal-to-noise ratios ranged from 10/1 at small angles to 25/1 at the larger angles. The background count level was significantly lower for "negative angles" than for "positive angles" (due to the nonsymmetrical geometry of the apparatus). In our calculations the data from 0 to -70° was more heavily weighted than that from 0 to $+70^\circ$, although the results were symmetrical for all gases studied.

To determine atomic-oxygen cross sections the ratio of the number density of O_2 in the beam during a mixture (O + O_2) run to that in the beam during a pure O_2 run was needed, as discussed below. This ratio was determined by measuring the mass 32 signal with the quadrupole mass spectrometer both before and after every O_2 and O + O_2 run. A mixture run was always followed immediately by a pure O_2 run, so that the conditions in the elec-

tron source and collectors were as close as possible for these two runs.

III. DATA, CORRECTIONS, AND RESULT REDUCTION

Since, in most cases, several independent readings were taken at a given angle, it was necessary to use some normalizing and averaging procedure. First, the individual signals D_i were linearly normalized to the same molecular-beam number density, electron-beam current, and, when necessary, dead time of the detection electronics to give $D_{\text{corr},i}$. Since the statistical noise is proportional to the square root of the total counts, or count time, each run was weighted by $w_i \equiv 1/(A+B)^{1/2}$ in obtaining the average corrected signal at each angle:

$$\bar{D}_{\text{corr}} \equiv \left(\sum_{i=1}^n w_i D_{\text{corr},i} + \sum_{i=n+1}^m w_i D_{\text{corr},i} \right) / \sum_{i=1}^m w_i, \quad (1)$$

where there are n data points at the positive angle (\sum_+) and $m-n$ data points at the corresponding negative angle (\sum_-).

To obtain the differential cross section, $d\sigma/d\Omega$,

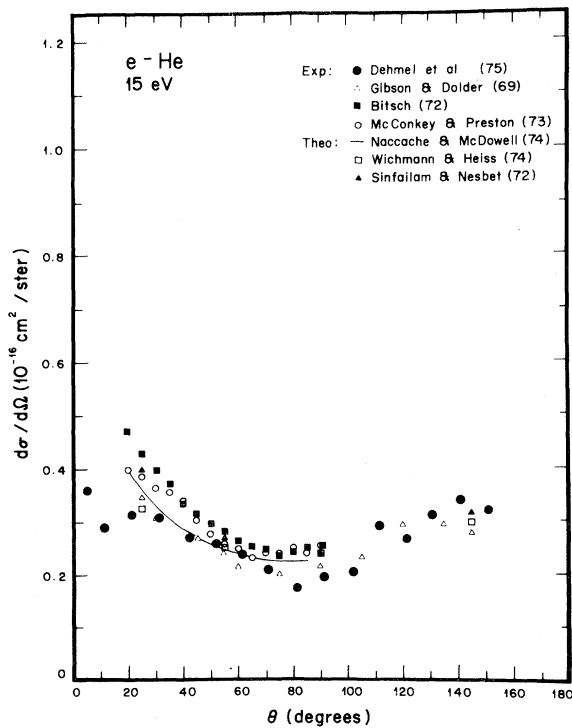


FIG. 3. Differential cross sections for the scattering of 15-eV electrons from He as a function of angle. Present results are compared to other experimental and theoretical results. In all graphs, numbers in parentheses following author's names represent year of publication. See references for sources of these data.

we first note that it is related to our signal counts \bar{D}_{corr} by an experimental scale factor k ,

$$\bar{D}_{\text{corr}}(\theta) = k[d\sigma(\theta)/d\Omega];$$

where k includes factors for the electron current, beam density, scattering path length, and the detector solid angle and efficiency factor. The scale factor was obtained from the total cross section, σ_T , since

$$k = 2\pi \int_0^\pi \bar{D}_{\text{corr}}(\theta) \sin\theta d\theta / \sigma_T. \quad (2)$$

Assuming a constant k implies that the effective product of path length and detector solid angle is independent of scattered angle. While this is not true in general,¹¹ it is a good assumption for our experimental geometry wherein the scattering volume is small ($\sim 0.025 \text{ cm}^3$), fixed by the intersection of the electron and molecular beams and well within the view angle of the detector at all angles. We have calculated a maximum error less than 2% due to this assumption for the angles reported below, which is well within our reproducibility.

The integral in Eq. (2) was obtained graphically with a planimeter by plotting $\bar{D}(\theta) \sin\theta$ versus θ ; this choice of variables gives us the correct end points of

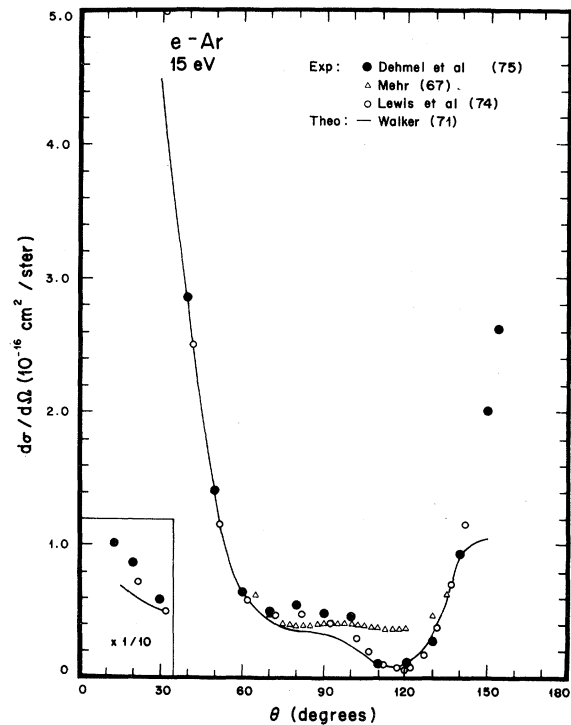


FIG. 4. Differential cross sections for the scattering of 15-eV electrons from Ar as a function of angle. Present results are compared to other experimental and theoretical results.

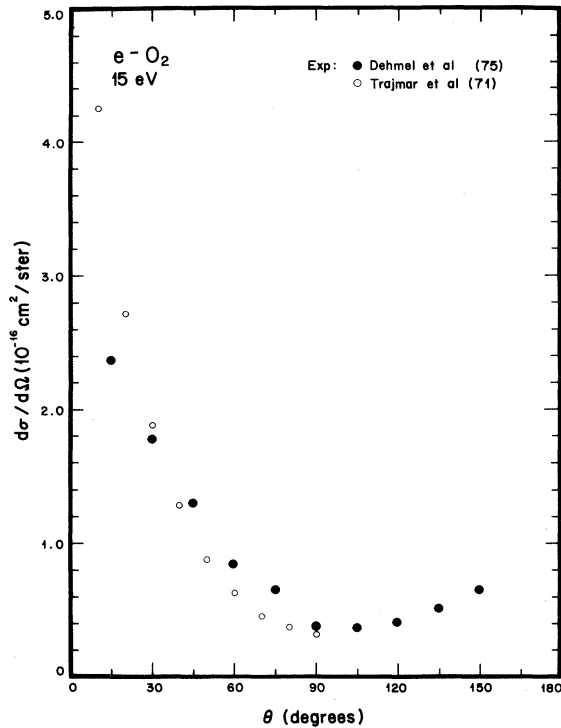


FIG. 5. Differential cross sections for the scattering of 15-eV electrons from O_2 as a function of angle. Present results are compared to experimental results of Trajmar *et al.* (Ref. 24).

the integration since $\sin\theta \rightarrow 0$ at 0° and 180° , where data are difficult to obtain. Total cross sections from the literature were then used to calculate k and then $d\sigma(\theta)/d\Omega = k^{-1}\bar{D}_{\text{corr}}(\theta)$. The total cross sections to which our data are thus normalized are (in units of 10^{-16} cm^2) 3.2, 19, 9.5, and 8 for He,¹² Ar,¹³ O_2 ,^{14,26} and ^{14}O at 15 eV and 7.0 and 7.5 for $^{26}O_2$ and ^{14}O at 5 eV.

For atomic oxygen, the scattered electron signal $D(O; \theta)$ had to be extracted from data for both the scattered electron signal measured for the $O-O_2$ mixture $D(O+O_2; \theta)$, and for the pure O_2 , $D(O_2; \theta)$. In order to get $D(O; \theta)$ the ratio γ of the number density of O_2 in the beam with the discharge on to that in the beam with the discharge off must be known. The relationship is

$$D(O; \theta) = D(O+O_2; \theta) - \gamma D(O_2; \theta). \quad (3)$$

γ was determined from the ratio of O_2^+ ion currents in the mass spectrometer with the discharge on (mixture) and discharge off (pure O_2 run). As mentioned above, each mixture run was immediately followed by a pure O_2 run.

The errors in our cross sections are obviously related to the errors in the total cross sections we used. Our own reproducibility was within 10%

for most cases, except for He below 15° and for atomic oxygen. For atomic oxygen, the error in γ is significant and we feel our reproducibility in the cross sections is better than 20% in most cases. The results for the gases studied at 5 and 15 eV are shown in Figs. 3–8.

IV. RESULTS AND DISCUSSION

Differential cross sections were obtained for He and Ar at 15 eV to establish the reliability of our apparatus and method of data reduction by a comparison with both experimental and theoretical results of other studies. For both gases the agreement is good. In Fig. 3 our results for He are shown with the experimental points of Gibson and Dolder,¹⁵ Bitsch,¹⁶ and McConkey and Preston,¹⁷ and the theoretical calculations of Naccache and McDowell,¹⁸ Wichmann and Heiss,¹⁹ and Sinfailam and Nesbet.²⁰ The experimental points of McConkey and Preston and of Bitsch were those as reported by Naccache and McDowell. The data of Sinfailam and Nesbet were computed as cross sections by Wichmann and Heiss. It is seen that there is good agreement with other reported data. The minimum at $\sim 80^\circ$ agrees with Gibson and

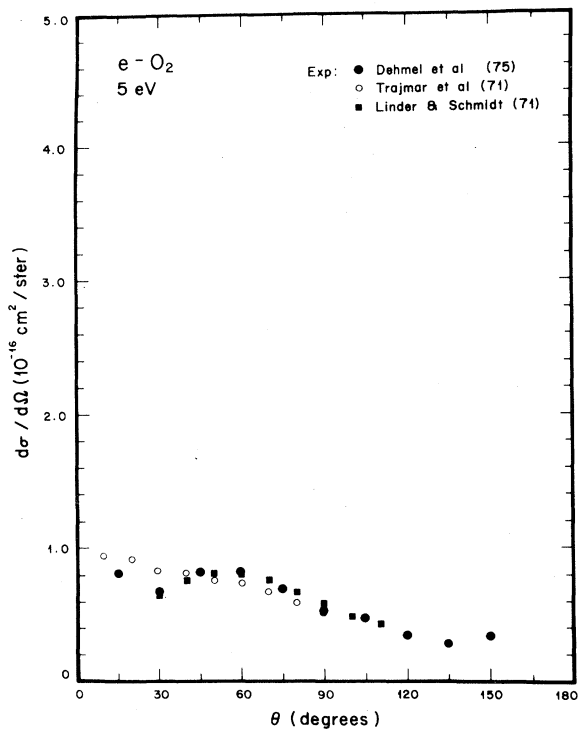


FIG. 6. Differential cross sections for the scattering of 5-eV electrons from O_2 as a function of angle. Present results (elastic+inelastic) are compared to experimental results of Trajmar *et al.* (Ref. 24) (elastic); (+) Linder and Schmidt (Ref. 25) (elastic, 4.0 eV).

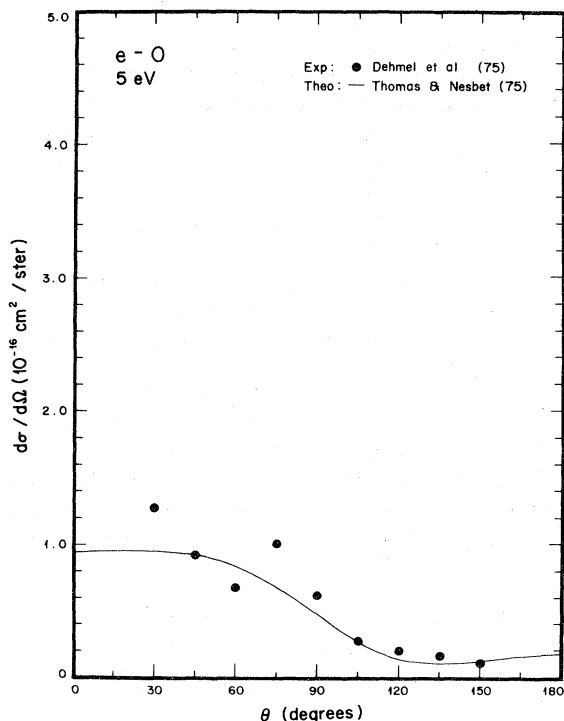


FIG. 7. Differential cross sections for the scattering of 5-eV electrons from O as a function of angle. Present results are compared to theoretical calculations of Thomas and Nesbet (Ref. 2) (elastic, 4.9 eV).

Dolder's data. Our small-angle points show a flatter behavior below 30° than do the others. However, the data below 15° is not as reliable due to noise from the primary electron beam.

Figure 4 compares our results for Ar with the experimental relative cross sections of Mehr²¹ and Lewis *et al.*²² and the theoretical curve of Walker.²³ These relative cross sections were normalized to ours for a best visual fit. We agree extremely well with Lewis *et al.*; the calculation of Walker is also quite good, giving the 115° minimum and the steeply rising behavior at small and large angles. The results of Mehr show a rather flat behavior from 75°–120° and do not show the pronounced minimum seen by others.

The present results for O₂ are compared with Trajmar *et al.*²⁴ at 15 eV in Fig. 5 and with Linder and Schmidt²⁵ (4 eV), and Trajmar *et al.*²⁴ at 5 eV in Fig. 6. For $\sigma_T(O_2)$ we have used, as did Trajmar, the total cross sections of Salop and Nakano.²⁶ Figure 5 shows that our 15-eV data agree to within 30% of Trajmar's, but our data show a slightly flatter behavior for angles less than 45°. Since they did not go above 90°, they did not see the minimum at ~105°. At 5 eV, Fig. 6 shows the three sets of data to be in good agreement, except that at 30° our data and that of Linder and Schmidt

show a slightly greater dip than does Trajmar *et al.* In both cases our data extend to larger scattering angles than previously reported data. We are not aware of any theoretical calculations for O₂ at these energies.

Figures 7 and 8 show our experimental results for O at 5 and 15 eV. These results are compared with the theoretical curves of Thomas and Nesbet² at 4.9 and 11.0 eV (their calculations were not carried out above this energy as it necessitated the inclusion of too many open channels for practical computation). The general features to be noted are (a) a main dip in the cross section which occurs at ~120° at both 5 and 15 eV; (b) a second dip which moves inward from 30° (15 eV) to 60° (5 eV); and (c) the large forward scattering at 5 eV; at 5 eV the backscattering does not increase with angle as it does at 15 eV.

It is seen that generally the theory for O is able to predict the magnitude of the cross section reasonably well at 5 eV and the main qualitative features of the backscattering behavior both at 5 eV and (as indicated by the 11-eV trend) at the higher energy including the decrease occurring around 90°–120°. However, the theory does not show the small-angle dip, which occurs at both 5 and 15 eV, nor does it seem, particularly at the higher energy,

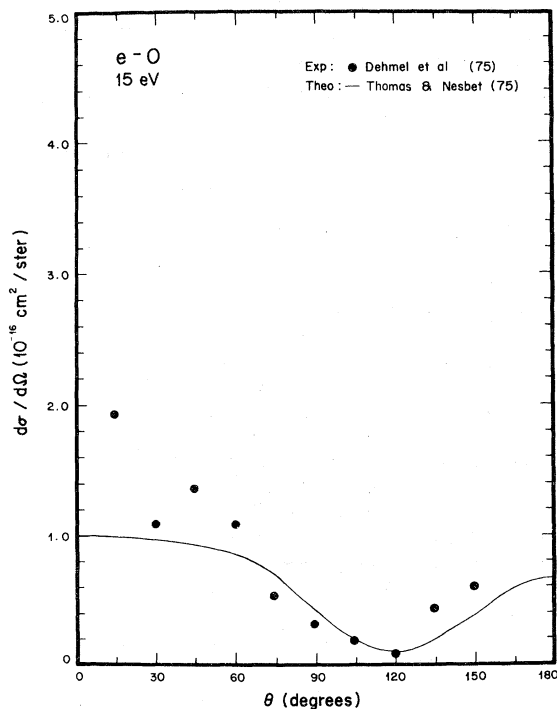


FIG. 8. Differential cross sections for the scattering of 15-eV electrons from O as a function of angle. Present results are compared to theoretical calculations of Thomas and Nesbet (Ref. 2) (elastic, 11.0 eV).

to show quite the proper small-angle slope. While we do not have as many data points around the dip as one would want, it was present in all runs and was not a consequence of our averaging procedures. It should be noted that "multiple dips" in the differential cross section are not at all unusual and appear in the low-energy scattering behavior of many gases (Ne, Ar, Kr, and Hg, for example).

As low-energy scattering is extremely sensitive to the polarization of the atom, it would seem reasonable that the target atom passes through a series of virtual excited states during the collision process. Thomas and Nesbet appear to have included all the higher-order partial waves of any importance (Sinfaillam and Nesbet²⁰); they included the channels $2s^2 2p^4$, $2s^1 2p^5$, and $2p^6$. Apparently, then, even higher excited states may be of importance to the scattering process, even at the lower energy (5 eV) examined here, and if included (difficult though the calculation may be) prediction of the experimentally observed forward-scattering behavior may be found.

In all cases, our results represent the sum of elastic plus inelastic cross sections. However, data available in the literature show that the total inelastic cross sections tend to be a factor 10^2 smaller than the elastic ones. In particular, the calculations of Thomas and Nesbet show the inelastic differential cross section for atomic oxygen to be (at its largest) less than 25% of the elastic cross section, and mostly a factor 10 or more

smaller than this.

The forward scattering to backscattering ratios for atomic oxygen were calculated by integrating our angular data points over the appropriate angles (20° – 88° , 92° – 160°) (extrapolation was carried out where necessary). The calculated ratio (4.1) is consistent with our directly measured¹ ratio data (5.0) at 5 eV, while at 15 eV the present experiment gives a higher ratio of 3.0 as compared to 1.72 (a lower bound) by direct measurement. Ratios for the other gases were also calculated and He (15 eV) gave good agreement, while the calculated results for Ar (15 eV) and O₂ (5 eV) were again (20–70)% higher than the previously reported lower bound. These results show that the ratio test is sensitive to the shape of the differential curve, and so, in its own way, is a simple and valuable test for theoretical angular calculations.

ACKNOWLEDGMENTS

We wish to thank John A. Rutherford and Intel-Com Rad Tech for making the electron-scattering apparatus available to us, and Edward K. Curley for helpful discussions on its operation. We are particularly grateful to Peter Poulsen who designed and built the microwave O source, and to Eugene Strein who assisted in the construction and testing of the scattered-electron detector. This research was supported by the National Science Foundation under grant No. ENG 71-02434A04.

*Present address: 20 Barnsdale Road, Short Hills, N.J. 07078.

†Visiting Professor on leave from the Department of Physics, Lycoming College, Williamsport, Penn.

¹R. C. Dehmel, M. A. Fineman, and D. R. Miller, *Phys. Rev. A* **9**, 1564 (1974).

²L. D. Thomas and R. K. Nesbet, *Phys. Rev. A* **11**, 170 (1975).

³L. J. Kieffer, *Bibliography of Low Energy Electron Collision Cross Section Data*, Natl. Bur. Std. Misc. Pub. No. 289 (U.S. GPO, Washington, D.C., 1967); update by G. E. Chamberlain and L. J. Kieffer, JILA Report No. 10, 1970 (unpublished); update through Dec. 1974, Nelson (private communication).

⁴R. C. Dehmel, Ph. D. thesis (University of California at San Diego, 1975) (unpublished).

⁵J. Anderson, R. Andres, and J. B. Fenn, *Adv. Chem. Phys.* **10**, 275 (1966).

⁶F. C. Fehsenfeld, K. M. Evenson, and H. P. Broida, *Rev. Sci. Instrum.* **36**, 294 (1965).

⁷D. Patch, Ph. D. thesis (University of California at San Diego, 1972) (unpublished).

⁸A. Falick, B. Mahan, and R. Myers, *J. Chem. Phys.* **42**, 1837 (1965).

⁹J. W. McGowan and E. M. Clarke, *Phys. Rev.* **167**, 43

(1968).

¹⁰J. W. McGowan, J. F. Williams, and E. K. Curley, *Phys. Rev.* **180**, 132 (1969).

¹¹C. E. Kuyatt, in *Methods of Experimental Physics*, edited by L. Marton (Vol. 7, Pt. A, p. 11) (Academic, New York, 1968).

¹²D. E. Golden and H. W. Bandel, *Phys. Rev.* **138**, A14 (1965).

¹³D. E. Golden and H. W. Bandel, *Phys. Rev.* **149**, 58 (1966).

¹⁴G. Sunshine, B. B. Aubrey, and B. Bederson, *Phys. Rev.* **154**, 1 (1967).

¹⁵J. R. Gibson and K. T. Dolder, *J. Phys. B* **2**, 1180 (1969).

¹⁶A. Bitsch, Ph. D. thesis (Trier-Kaiserlautern, 1972) (unpublished) (see Ref. 17 wherein his results are reported).

¹⁷T. W. McConkey and J. A. Preston, *J. Phys. B* **8**, 63 (1975).

¹⁸P. F. Naccache and M. R. C. McDowell, *J. Phys. B* **7**, 2203 (1974).

¹⁹E. Wichmann and P. Heiss, *J. Phys. B* **7**, 1042 (1974).

²⁰A. L. Sinfaillam and R. K. Nesbet, *Phys. Rev. A* **6**, 2118 (1972).

²¹J. Mehr, *Z. Phys.* **198**, 345 (1967).

²²B. R. Lewis, J. B. Furness, P. J. O. Teubner, and

- E. Weigold, *J. Phys. B* 7, 1083 (1974).
- ²³D. W. Walker, *Advan. Phys.* 20, 257 (1971).
- ²⁴S. Trajmar, D. C. Cartwright, and W. Williams, *Phys. Rev. A* 4, 1482 (1971).
- ²⁵F. Linder and H. Schmidt, *Z. Naturforsch.* 26a, 1617 (1971).
- ²⁶A. Salop and H. H. Nakano, *Phys. Rev. A* 2, 127 (1970).